Molecular Pharmacology Fast Forward. Published on March 21, 2017 as DOI: 10.1124/mol.117.108290
This article has not been copyedited and formatted. The final version may differ from this version.

ID MOLPHARM/2017/108290

Halogenated ether, alcohol, and alkane anesthetics activate TASK-3 tandem pore potassium channels likely through a common mechanism

Anita Luethy, James D. Boghosian, Rithu Srikantha, and Joseph F. Cotten

Department of Anesthesia, Critical Care, and Pain Medicine

Massachusetts General Hospital, Boston, MA 02114 (A.L., J.B., and J.F.C)

Department of Anesthesia, Kantonsspital Aarau, Aarau, Switzerland (A.L.)

Carver College of Medicine, University of Iowa, Iowa City, IA 52242 (R.S.)

Molecular Pharmacology Fast Forward. Published on March 21, 2017 as DOI: 10.1124/mol.117.108290
This article has not been copyedited and formatted. The final version may differ from this version.

Running Title Page

Activation of TASK-3 channels by multiple halogenated agents.

Correspondence: Joseph F. Cotten, M.D., PhD., Massachusetts General Hospital, Department of Anesthesia, Critical Care, and Pain Medicine, 55 Fruit Street, GRB 444, Boston, MA. 02114, Tel: (617) 726-8822, FAX: (617) 724-8644

E-mail: jcotten@mgh.harvard.edu

Number of text pages: 28

Number of tables: 0

Number of Figures: 10

Number of references: 37

Number of words in the *Abstract*: 248

Number of words in *Introduction*: 748

Number of words in *Discussion: 1476*

Abbreviations: FRT, fischer rat thyroid; TASK, TWIK-related acid-sensitive potassium channel; NEM, N-ethylmaleimide; TCE, 2,2,2-tricholoroethanol; DCE, 2,2-dichloroethanol; MCE, 2-chloroethanol; TBE, 2,2,2-tribromoethanol; CBr_4, carbon tetrabromide; CCl_4, carbon tetrachloride; $CHCl_3$, chloroform; CI_4, carbon tetraiodide; EtOH, ethanol; TFE, 2,2,2-

Molecular Pharmacology Fast Forward. Published on March 21, 2017 as DOI: 10.1124/mol.117.108290
This article has not been copyedited and formatted. The final version may differ from this version.

trifluoroethanol; m3 GPCR, m3 muscarinic G protein coupled receptor; TASK-3/TREK-1, 243-VLRFLT-248 => 243-GDWLRV-249; HFP, 1,1,1,3,3,3-hexafluoropropanol.

Molecular Pharmacology Fast Forward. Published on March 21, 2017 as DOI: 10.1124/mol.117.108290
This article has not been copyedited and formatted. The final version may differ from this version.

Abstract

TASK-3 (KCNK9) tandem pore potassium channel function is activated by halogenated anesthetics through binding at a putative anesthetic binding cavity. To understand pharmacological requirements for TASK-3 activation, we studied the concentration-response of TASK-3 to several anesthetics (isoflurane, desflurane, sevoflurane, halothane, α-chloralose, 2,2,2-trichloroethanol(TCE), and chloral hydrate), to ethanol, and to a panel of halogenated methanes and alcohols. We used mutagenesis to probe the anesthetic binding cavity as observed in a TASK-3 homology model. METHODS: TASK-3 activation was quantified by Ussing chamber voltage clamp analysis. We mutagenized residue Val-136, which lines the anesthetic binding cavity, its flanking residues (132 to 140), and Leu-122, a pore gating residue. RESULTS: 2-halogenated ethanols activate wild-type TASK-3 with the rank order efficacy (normalized current [95% confidence]): 2,2,2-tribromo-(267%[240-294]) > 2,2,2-trichloro-(215%[196-234]) > chloral hydrate(165%[161-176]) > 2,2-dichloro- > 2-chloro ≈ 2,2,2-trifluoroethanol > ethanol. Similarly, carbon tetrabromide(296%[245-346]), carbon tetrachloride(180%[163-196]) and 1,1,1,3,3,3-hexafluoropropanol(200%[194-206]) activate TASK-3, whereas the larger carbon tetraiodide and α-chloralose inhibit. Clinical agents activate TASK-3 with the following rank order efficacy: halothane(207%[202-212]) > isoflurane(169%[161-176]) > sevoflurane(164%[150-177]) > desflurane(119%[109-129]). Mutations at and near residue-136 modify TCE activation of TASK-3, and; interestingly, M159W, V136E, and L122D, were resistant to both isoflurane and TCE activation. CONCLUSIONS: TASK-3 function is activated by a multiple agents and requires a halogenated substituent between ~30 and 232 cm^3/mol volume with potency increased by halogen

Molecular Pharmacology Fast Forward. Published on March 21, 2017 as DOI: 10.1124/mol.117.108290
This article has not been copyedited and formatted. The final version may differ from this version.

polarizeability. Val-136 and adjacent residues may mediate anesthetic binding and stabilize an open state regulated by pore residue Leu-122. Isoflurane and TCE likely share commonalities in their mechanism of TASK-3 activation.

Molecular Pharmacology Fast Forward. Published on March 21, 2017 as DOI: 10.1124/mol.117.108290
This article has not been copyedited and formatted. The final version may differ from this version.

Introduction

The TASK-3(KCNK9) protein is a member of the tandem pore(K_{2p}) potassium channel family, a collection of fifteen channels that regulate neuronal excitability(Yost, 2003). TASK-3 function is inhibited by extracellular acidic pH and by activation of $G\alpha_{Q/11}$-coupled G protein coupled receptors(GPCRs), which are involved in CNS arousal and consciousness (e.g., orexin, muscarinic, adrenergic, and histamine receptors)(Franks, 2008; Talley and Bayliss, 2002). TASK-3 and other tandem pore channel functions are activated by halogenated volatile anesthetics, which causes neuronal hyperpolarization and quiescence(Conway and Cotten, 2012; Franks and Lieb, 1988; Patel et al., 1999); and, therefore, tandem pore channels may mediate some aspects of anesthesia. Importantly, knockout mice lacking TASK-3 channels or TREK-1 channels, also a tandem pore member, are resistant to halothane- and isoflurane-induced loss of righting and immobility(Heurteaux et al., 2004; Lazarenko et al., 2010; Pang et al., 2009).

The mechanisms of TASK-3 activation by anesthetics and the drug structural requirements necessary to activate TASK-3 are minimally understood. TASK-3 activation studies have been limited to several clinical anesthetics: TASK-3 is activated by isoflurane, halothane, and chloroform; conversely, TASK-3 is unaffected by non-halogenated nitrous oxide, cyclopropane, propofol, and xenon and is inhibited by local anesthetics (e.g., bupivicaine)(Andres-Enguix et al., 2007; Gruss et al., 2004; Kindler et al., 1999; Talley and Bayliss, 2002). Trichloroethanol (TCE), an active metabolite of the hypnotic chloral hydrate, a $GABA_A$ chloride channel activator, activates TREK-1 and TRAAK tandem pore potassium channels(Harinath and Sikdar, 2004; Krasowski et al., 1998; Krasowski and Harrison, 2000; Parelkar et al., 2010). The effects of TCE on TASK-3 have not been reported.

Molecular Pharmacology Fast Forward. Published on March 21, 2017 as DOI: 10.1124/mol.117.108290
This article has not been copyedited and formatted. The final version may differ from this version.

Molecular chimerae and mutagenesis studies have identified TASK-3 mutants that are resistant to activation by halogenated anesthetics. Mutants involve residues Met-159 and 243-VLRFLT-248 (a.k.a. "TASK-3/TREK-1" mutant) in the intracellular portions of transmembrane domains 3 and 4, respectively (Fig. 1)(Andres-Enguix et al., 2007; Patel et al., 1999; Talley and Bayliss, 2002). Notably, covalent modification of a cysteine residue introduced at TASK-3 residue-159 (M159C) causes channel activation, suggesting perturbations in this "pocket" activate TASK-3(Conway and Cotten, 2012). Tandem pore channel crystal structures for TWIK-1, TRAAK, and TREK-2 have been solved and have enabled homology model construction(Brohawn et al., 2012; Dong et al., 2015; Lolicato et al., 2014; Miller and Long, 2012). In a LyTASK homology model, residues 159 and 243 through 248 contribute to an "anesthetic binding pocket"(Bertaccini et al., 2014). Additionally, mutations at residues Leu-241, Leu-242, and Ser-155 (i.e., L241A, L242A, and S155W), near/in the "binding pocket" also modify halothane activation. TASK-3 and LyTASK share 47% amino acid identity, and the anesthetic binding pocket is apparent in our TASK-3 homology structure (Fig. 1B and Supplementary Fig. S1). Val-136 in TASK-3, a hydrophobic residue, is conspicuous in its proximity to residues-159 and -243 and as a component of the "anesthetic pocket's" inner wall (Fig. 1B).

Excised, single channel patch clamp studies demonstrate that anesthetics activate tandem pore channels through gating effects, and not through surface expression or single channel conductance(Patel et al., 1999; Winegar and Yost, 1998). Although the mechanism of gating in TASK-3 is unknown, functional and crystallographic studies in related channels are notable. TREK-1 studies demonstrate a "C-type" gating mechanism involving residues near the selectivity filter. Both TRAAK and TREK-2 have been crystallized in presumed conducting and

Molecular Pharmacology Fast Forward. Published on March 21, 2017 as DOI: 10.1124/mol.117.108290
This article has not been copyedited and formatted. The final version may differ from this version.

non-conducting conformations, with structural changes centered around the intracellular portions of transmembrane domains 2, 3, and 4(Brohawn et al., 2014; Dong et al., 2015; Lolicato et al., 2014). Finally, hydrophobic residues in the pore of the TWIK-1 tandem pore channel (e.g., Leu-146) have a critical role in gating. Polar mutations at this residue cause channel activation, and modeling studies suggest the mechanism may be through effects on pore hydration essential for potassium conductance (Aryal et al., 2014). Residue Leu-122 in TASK-3 aligns with Leu-146 of TWIK-1; and, in our TASK-3 homology model, Leu-122 lines both the pore and the fenestration (Fig. 1).

In this study, we had three objectives. First, we determined that TCE activates TASK-3 and examined TASK-3 activation by a series of halogenated alcohols and related compounds to understand drug structural requirements for activation. Second, we hypothesized that mutants resistant to isoflurane activation would be similarly resistant to activation by TCE or by NEM-modification of Cys-159 implying commonalities in their mechanisms of action. Third, we hypothesized that Val-136 contributes to anesthetic binding and transmits changes in the "anesthetic binding pocket" to the pore residue, Leu-122. To test this hypothesis we mutagenized Val-136 and adjacent residues, as well as Leu-122, and studied effects on TASK-3 activation by TCE and in some cases isoflurane.

Molecular Pharmacology Fast Forward. Published on March 21, 2017 as DOI: 10.1124/mol.117.108290
This article has not been copyedited and formatted. The final version may differ from this version.

Materials and Methods

Molecular biology -- For electrophysiology studies, rat TASK-3, rat TASK-1, and LyTASK were cloned into variants of the pcDNA3.1 vector (Invitrogen, Carlsbad, CA). Rat TASK-1 had residues 312 to 331 deleted to promote surface expression (Renigunta et al. Traffic 2006). Directed missense mutations were introduced into cDNAs using the "QuikChange" method of mutagenesis (Phusion HF Mastermix, New England Biolabs, Ipswich, MA). All mutant cDNA were sequenced bidirectionally (MGH DNA Core Facility). pYesMet25 yeast expression vector encoding yeast Trk1p or a non-functional Kir 2.1 "stuffer" cDNA were a generous gift from Prof. Dan Minor (UCSF, San Francisco, CA). For our studies, we ligated wild-type TASK-3 or randomly mutagenized TASK3 (see below) cDNA into pYesMet25 employing a yeast Kozak sequence (AAAAA).

Cell culture, transfection, and Ussing chamber studies -- Fischer rat thyroid (FRT) epithelial cells were maintained in Ham's F-12 media supplemented with 5% fetal calf serum (Sigma-Aldrich, St. Louis, MO) at 37°C and 5% CO2 in a humidified incubator. After trypsinization, cells were cultured on semipermeable supports (~1.5 x 10^5 cells per support; Corning Snapwell polycarbonate; 0.4 μm pore size; 12 mm diameter; Fisher Scientific, Pittsburgh, PA) and transfected in suspension with Lipofectamine 2000 (Invitrogen, Carlsbad, CA). Monolayers were studied 48 to 72 h after transfection.

Electrophysiology methods were based on that of (Sheppard et al., 1994). Before placing a study monolayer in the chamber, junction potentials were zeroed using a "dummy" membrane. A potassium gradient was applied across the study monolayer (basolateral > apical) and the transepithelial voltage clamped at 0 mV (DVC-1000 amplifier, World Precision Instruments, Sarasota, FL). The apical bathing solution was (in mM): 135 NaCl, 1.2 $MgCl_2$, 1.2 $CaCl_2$, 10

Molecular Pharmacology Fast Forward. Published on March 21, 2017 as DOI: 10.1124/mol.117.108290
This article has not been copyedited and formatted. The final version may differ from this version.

HEPES, 10 Dextrose, pH 7.4 with NaOH; the basolateral bathing was solution (in mM): 135 KCl, 1.2 $MgCl_2$, 1.2 $CaCl_2$, 10 HEPES, 10 Dextrose, pH 7.4 with KOH. MES was used in lieu of HEPES in the pH 5.5 apical solution. The Ussing chamber current signal was amplified and digitized (10 Hz) with a USB-6009 data acquisition board (National Instruments, Austin, TX) interfaced with an Apple Computer running Labview 8.5 software (National Instruments). Potassium current data were averaged every 1 sec for analysis. By convention, positive current indicates positive charge flowing in the basolateral to apical direction; total current through the 1.2 cm^2 monolayer is reported in the figures. Transepithelial voltage pulses (+5 mV and of 1 sec duration), referenced to the apical surface, were applied intermittently to assess transepithelial resistance and monolayer integrity. Air was continuously bubbled through apical and basolateral solutions for mixing purposes. All studies were conducted at room temperature (22-24°C). Isoflurane, desflurane, sevoflurane, and halothane were applied using agent specific variable bypass vaporizers in series with gas flow providing mixing bubbles to the Ussing chamber. A calibrated Datex Capnomac Ultima medical gas analyzer (GE Healthcare) quantified the concentration in the gas phase (in % atmosphere) and was converted to a solute concentration (in mM) using methods described by Franks and Lieb (1993) with Ostwald partition coefficients (22°C) of 1.57 (halothane), 1.21 (isoflurane), 0.42 (sevoflurane), and 0.29 (desflurane) (Honemann et al., 1998).

Yeast growth studies -- The potassium-sensitive trk1Δtrk2Δ *Saccharomyces cerevisiae* yeast strain (R5421: ura3-52 his3Δ200 leu2Δ1 trp1Δ1 ade2 trk1Δ::HIS3 trk2Δ::HIS3) was a generous gift from Prof. Richard Gaber (Northwestern University, Evanston, IL). Yeast plasmid DNA transformations were conducted using the Yeastmaker Yeast Transformation System 2 (Clontech, Mountain View, CA) or using the Frozen-EZ Yeast Transformation Kit (Zymo

Molecular Pharmacology Fast Forward. Published on March 21, 2017 as DOI: 10.1124/mol.117.108290
This article has not been copyedited and formatted. The final version may differ from this version.

Research, Irvine, CA). Wild-type TASK-3, which fails to rescue the potassium-sensitive growth phenotype of trk1Δtrk2Δ yeast, was optimized for functional expression in yeast by mutagenic PCR (Cadwell and Joyce, 2006). The "yeast optimized" TASK-3 cDNA clone was transformed into yeast and was identified by growth on low potassium agarose plates after replica plating. "Yeast optimized" TASK-3 cDNA encodes the following six missense mutations: T17I, D27E, D32G, K79E, F202L, and F246Y. The optimized channel remains functional in FRT monolayers and provides potassium current levels similar to the wild-type TASK-3 channel (Supplementary Fig. S4). Additionally, it remains inhibited by extracellular acidic pH, is activated by TBE and is inhibited by m3 GPCR activation (n = 3; data not shown). Supplementary Fig. S5 demonstrates the potassium sensitivity of the trk1Δtrk2Δ yeast strain, and its phenotypic rescue by Trk1p and "yeast optimized" wild-type TASK-3 and less so by wild-type TASK-3 and a non-functioning Kir 2.1 "stuffer" potassium channel. For these studies, following transformation and plating on high potassium (100 mM KCl-added) -Ura/-Met/-His selective agar plates, 5 clones of trk1Δtrk2Δ yeast transformed with each plasmid were combined, grown up in high potassium selective media, pelleted, washed with sterile water to remove excess potassium, and resuspended in low potassium (no added potassium) or high potassium -Ura/-Met/-His liquid media (US Biological, Salem, MA) at a 650 nM light absorbance (A650) of ~0.01. After dilution, cells were cultured at 30°C in 96 well format with continuous shaking on a Titer Plate Shaker (Model 4625, Lab-Line Instruments/Thermo Fisher Scientific, Waltham, MA). Growth was measured intermittently by A650 nm analysis using a SpectraMAX 190 plate reader (Molecular Devices, Sunnyvale, CA). For TBE selection studies, yeast expressing "yeast optimized" wild-type TASK-3 and "yeast optimized" TASK-3 V136E were cultured in high potassium selective synthetic liquid media (-Ura/-Met/-His) at 30°C to a

Molecular Pharmacology Fast Forward. Published on March 21, 2017 as DOI: 10.1124/mol.117.108290
This article has not been copyedited and formatted. The final version may differ from this version.

600 nM light absorbance (A600) ~1.0 (P330 Nanophotometer, Implen, Westlake Village, CA). Yeast were pelleted and washed, re-suspended, mixed 1:1 (wild-type:V136E), diluted to an A600 of ~0.01, and re-grown in a 5 ml volume liquid culture in the presence or absence of 1 mM TBE at 30°C in low potassium selective synthetic media (-Ura/-Met/-His). After growth to an A600 ~1.0, yeast were pelleted by centrifugation, plasmid DNA was recovered (QIAprep Spin Miniprep kit, Qiagen, Germantown, MD), and the sequence flanking residue-136 was amplified by PCR. After gel purification, PCR fragments were subjected to MiSeq Next Generation Sequencing (2 x 150 bp; Illumina, San Diego, CA) in the MGH DNA Core, and custom computer software script written in Python was used to analyze the sequencing data and to count the frequency of Val-136 relative to Glu-136 in each sample.

Graphing, statistical analysis, chemical structure analysis and homology model -- Microsoft Excel (Microsoft, Redmond, WA), Prism 5.0b (GraphPad Software, La Jolla, CA), and Adobe Illustrator (Adobe Systems, San Jose, CA) were used for data/statistical analysis, graphing, regression, and figure preparation. A one-way analysis of variance and a post hoc Bonferroni multiple comparison test or a Student's t test were used to compare group means as indicated in the figure legends or text. Molecular structures, graphics, and analyses were performed with the UCSF Chimera software package and ChemDoodle/ChemDoodle 3D (iChemLabs, Somerset, NJ). Chimera software was developed by the Resource for Biocomputing, Visualization, and Informatics at the University of California, San Francisco (supported by NIGMS P41-GM103311)(Pettersen et al., 2004). Molecular volume were calculated with Chimera; XlogP, and polarizability were estimated using ChemDoodle (iChemLabs). The TASK-3 homology (Fig. 1) was developed as previously described and is based on the PDB 3UKM (TWIK-1 channel) structure (Chokshi et al., 2015; Miller and Long,

Molecular Pharmacology Fast Forward. Published on March 21, 2017 as DOI: 10.1124/mol.117.108290
This article has not been copyedited and formatted. The final version may differ from this version.

2012).

Reagents -- All chemicals and supplies and reagents were obtained from Sigma-Aldrich or Fisher Scientific. NEM, carbon tetrabromide and carbon tetraiodide were solubilized in DMSO. TASK-3 function is minimally affected by DMSO at final bath concentrations up to 2% (normalized current of 100±1.1%; n = 3); and concentration-response studies remained at or below this level.

Molecular Pharmacology Fast Forward. Published on March 21, 2017 as DOI: 10.1124/mol.117.108290
This article has not been copyedited and formatted. The final version may differ from this version.

Results

Halogenated ethers, alcohols, and alkanes activate TASK-3 potassium channel function -- Rat TASK-3 was transiently expressed in FRT cell monolayers, which provides a large, positive, pH-inhibited transepithelial potassium current not otherwise present in FRT monolayers. The TASK-3 potassium current was activated by a range of halogenated compounds (Fig. 2, 3, and 4) including 2,2,2-trichloroethanol (TCE). Ethanol (without halogenation) (Fig. 3) provided no activation at similar concentrations, suggesting it is the halogenated 2-carbon on the various ethanol derivatives that engages the channel. Consistent with this, carbon tetrabromide (CBr_4) and carbon tetrachloride (CCl_4) both activate TASK-3 (Fig. 3). Of all the agents studied, CBr_4 had the highest potency (EC_{50} ~ 16 μM) and efficacy (normalized current of ~296%) for wild-type TASK-3 activation (Fig. 3). Clinically relevant agents chloral hydrate, halothane, isoflurane, sevoflurane, and desflurane all activate TASK-3; and, of these, halothane and desflurane were the most and least effective, respectively (Fig. 4). Interestingly, 1,1,1,3,3,3-hexafluoropropanol (HFP; Fig. 2), a component of sevoflurane, activates like sevoflurane (Fig. 4), but with ~5-fold lower potency. Notably, the largest agents, carbon tetraiodide and α-chloralose, as well as the smallest (e.g., ethanol, MCE, TFE, isoamyl alcohol), failed to or minimally activated TASK-3 (Figs. 3 and 4).

TASK-3 homologs, Lymnaea TASK (LyTASK) and TASK-1, were both activated by halogenated ethanols with a greater efficacy than that of wild-type TASK-3 (Supplementary Fig. S2; LyTASK: 708±47% (n=5) normalized current at 5 mM TBE and 1054±248% (n = 4) at 20 mM TCE; TASK-1: 3531±2845% (n=3) at 4.4 mM TBE). The concentration-response curves for both channels, however, were right-shifted relative to wild-type TASK-3, suggesting a lower

Molecular Pharmacology Fast Forward. Published on March 21, 2017 as DOI: 10.1124/mol.117.108290
This article has not been copyedited and formatted. The final version may differ from this version.

binding affinity to the activating compounds relative to TASK-3 (Supplementary Fig. S2D). The very small basal currents provided by TASK-1 (1.6±1.1 μA; n = 3) contributed significant variability to our TASK-1 results.

Amino acids both in the anesthetic binding pocket and in the pore are required for TASK-3 activation -- Val-136 resides in close proximity to Met-159 and lines a putative anesthetic binding pocket in TASK-3 (Fig. 1). Mutagenesis of residue-136 to various residues impairs TCE activation (Fig. 5; Supplementary Fig. S3). Because introduction of a charged aspartate residue in the putative anesthetic binding pocket should impair TASK-3 interactions with the hydrophobic trichloromethane substituent of TCE, we undertook scanning aspartate mutagenesis of residues adjacent to 136 in the primary amino acid sequence (132 to 140). Residues-133, -139, and -140, each approximately one helical turn from 136 and predicted to line the anesthetic pocket (Figs. 1 and 5C), when mutated, modify TCE activation.

Because Leu-122 resides on the same transmembrane domain as Val-136 (Fig. 1), and since an equivalent residue in the TWIK-1 channel pore (Leu-146) has a putative role in gating, we studied the effect of Leu-122 mutation on TASK-3 activation. Interestingly, the L122D mutation completely eliminates activation by both isoflurane and TCE (Fig. 6 and Supplementary Fig. S3). From prior work, we know mutations at TASK-3 residue-159 (e.g., M159W) impair activation by halogenated volatile anesthetics such as isoflurane (Andres-Enguix et al., 2007; Conway and Cotten, 2012). In the current study, we observed that M159W is similarly resistant to TCE activation (Fig. 6 and Supplementary Fig. S3).

NEM-modification of Cys-159 in the TASK-3 M159C mutant causes marked channel activation. NEM is an uncharged, membrane-permeant, thiol-selective alkylating agent with minimal effects on wild-type TASK-3 function (Conway and Cotten, 2012). We studied the

Molecular Pharmacology Fast Forward. Published on March 21, 2017 as DOI: 10.1124/mol.117.108290
This article has not been copyedited and formatted. The final version may differ from this version.

effect of L122D and V136E on this process by preparing the following double mutants, L122D/M159C and V136E/M159C, and quantifying the extent of activation by 5 mM NEM (Fig. 7). L122D and V136E mutations both impaired 5 mM NEM activation; the smaller residual response to NEM suggest Cys-159 is still alkylated in both double mutants (Fig. 7). Like wild-type TASK-3, the function of single mutants TASK-3 L122D and V136E are minimally impacted by 5 mM NEM exposure of the same duration (L122D: 100±1% normalized current, n=3; V136E: 89±4%, n=3).

TASK-3 V136E, unlike L122D and N133D, retains sensitivity to m3 muscarinic GPCR inhibition -- TASK-3 channels are inhibited by $G\alpha_{Q/11}$-coupled GPCRs, and several anesthetic-resistant mutant TASK-3 channels are resistant to this GPCR regulation, including M159W, NEM-modified M159C, and TASK-3/TREK-1 channels in which residues 243 to 248 (VLRFLT) are mutated to GDWLRV (Conway and Cotten, 2012; Talley and Bayliss, 2002). To explore the effects of L122D, N133D, V136E, and L140D mutations on TASK-3 GPCR regulation, we studied each mutant's functional response to activation of a co-expressed m3 GPCR. Carbachol, an m3 GPCR agonist, inhibited potassium currents in V136E/m3 GPCR and in wild-type TASK-3/m3 GPCR expressing monolayers to a similar extent (Fig. 8). Currents through TASK-3 L122D and N133D channels, however, were completely resistant to GPCR regulation; although they remained sensitive to inhibition by extracellular pH (Fig. 8). The L140D mutant was somewhat resistant to GPCR regulation.

2,2,2-tribromoethanol (TBE) selects for wild-type TASK-3 over V136E TASK-3 expressed in trk1Δtrk2Δ potassium-sensitive yeast -- *Saccharomyces cerevisiae* yeast lacking Trk1p and Trk2p potassium transporters (trk1Δtrk2Δ) require supplemental potassium (e.g., 100 mM KCl) for growth. Heterologous potassium channel expression, however, rescues their

Molecular Pharmacology Fast Forward. Published on March 21, 2017 as DOI: 10.1124/mol.117.108290
This article has not been copyedited and formatted. The final version may differ from this version.

phenotype to permit growth in low potassium media (Supplementary Fig. S5), which enables their use in high throughput pharmacologic and mutagenic potassium channel screens (Bagriantsev and Minor, 2013; Nakamura and Gaber, 1998). To validate our electrophysiology findings in a different system, trk1Δtrk2Δ yeast were transformed with "yeast optimized" (see Methods) wild-type TASK-3 (containing Val-136) or V136E TASK-3 cDNA and mixed in 1:1 ratio (wild-type:V136E) for culture in low potassium media in the presence or absence of 1 mM TBE. Following growth to an A600 > 1.0, plasmid DNA was isolated from the cultures and the relative frequency of each TASK-3 variant (Val-136 or Glu-136 containing) were counted by next generation sequencing. Supplementary Fig. S6 shows that yeast grew more slowly in the presence of 1 mM TBE taking 5.7 versus 2.8 days to reach an A600 > 1.0. Fig. 9, however, shows that TBE enriched the relative frequency of wild-type TASK-3 over that of TASK-3 V136E.

Discussion

In this study we measured the concentration-response of several halogenated alcohols, alkanes, and ethers on TASK-3 channel function and identified several new potent and effective TASK-3, LyTASK, and TASK-1 activating compounds (e.g., TCE, TBE, CCl_4, and CBr_4). Guided by a TASK-3 homology model, we identified several residues (e.g., 133, 136, 139, and 140) predicted to line a putative anesthetic binding pocket -- first described in the LyTASK potassium channel homolog -- that, when mutated, modify TCE and isoflurane activation of TASK-3 or NEM activation of TASK-3 M159C. Finally, we identified Leu-122, a putative gating residue in the channel pore, that when mutated (L122D) renders TASK-3 resistant to activation by TCE, isoflurane, and NEM and to inhibition by activated m3 GPCRs.

Molecular Pharmacology Fast Forward. Published on March 21, 2017 as DOI: 10.1124/mol.117.108290
This article has not been copyedited and formatted. The final version may differ from this version.

Drug attributes required for TASK-3 activation -- We determined halogenated agents (alcohols, alkanes, and ethers) activate TASK-3. It is likely the halogenated 2-carbon of ethanolic agents that engages the channel to promote activation (Fig. 10) and not the hydroxylated 1-carbon, since non-halogenated ethanol fails to activate TASK-3 and because both CBr_4 and CCl_4 cause TASK-3 activation (Fig. 3). The degree (e.g., mono-, di-, vs. trichloroethanol) and type of halogenation (e.g., fluorine, chlorine, vs. bromine) at the 2-carbon influences activation potency and efficacy (Fig. 3). Halogenation has at least 3 effects on the molecule: 1) increased volume, 2) increased polarizeability, and 3) increased hydrophobicity. We used fluoro-, chloro-, bromo-, and iodoform chemical structures as surrogates to estimate the physicochemical properties of the halogenated 2-carbon substituent (Fig. 2C). From these, we speculate a 2-carbon size between 30.31 (from fluoroform) and 232.0 cm^3/mol (from iodoform) may be required to support TASK-3 activation (Fig. 2). Like the alcohols (Fig. 10), we speculate only a portion of the larger halogenated ether/alkane molecules binds within the TASK-3 "binding cavity", such as the hexafluoropropane substituent of sevoflurane (Fig. 2). The increased potency of halogenated methanes relative to the similarly halogenated ethanols (e.g., EC_{50} of 1077 vs. 289 μM for TCE vs. CCl_4 and 295 vs. 16 μM for TBE vs. CBr_4) may be due to symmetry, as the methanes engage the channel in an identical manner regardless of orientation. An alcohol must orient itself to enter the binding site; additionally, the 1-carbon hydroxyl may favor solvation in an aqueous environment (Fig. 10). Interestingly, chloral hydrate (Fig. 2), which contains an additional hydroxyl group, is less potent than TCE (EC_{50} of 7141 vs. 1077 μM, respectively). Increased substituent polarizeability may also enhance potency: for example, CBr_4 is more potent than CCl_4 (EC_{50} of 16 vs. 289 μM), and TCE is more potent than the similarly-sized and similarly-effective TASK-3 activator HFP (EC_{50} of 1077 vs. 1942 μM),

Molecular Pharmacology Fast Forward. Published on March 21, 2017 as DOI: 10.1124/mol.117.108290
This article has not been copyedited and formatted. The final version may differ from this version.

despite its increased hydrophobicity (XlogP 3.088 vs. 3.418; Fig. 2C). As reference, bromoform, chloroform, and hexafluoropropane have estimated polarizabilities of 12, 8.5, and 6.6 $Å^3$ (Fig. 2C). Crystallographic studies of protein-halogenated anesthetic complexes demonstrated polarization of the hydrophobic anesthetic molecules to accommodate polar and non-polar interactions within amphiphilic binding cavities(Bertaccini et al., 2007). The putative cavity in TASK-3 (Supplementary Fig. S1) is largely hydrophobic with some polar characteristics provided by Ser-155 and Met-159. The hypnotic potency of several halogenated compounds used in this study are shown in Supplementary Table S1 for reference.

From this data and the work of others, it is known that several anesthetic agents fail to activate TASK-3 including ethanol, xenon, nitrous oxide, propofol, etomidate (personal observation), cyclopropane, carbon tetraiodide, and α-chloralose(Gruss et al., 2004; Putzke et al., 2007). Given our current findings, we speculate these compounds may lack overall volume or lack a hydrophobic, polarizeable substituent of suitable volume (e.g., tribromo-methyl of TBE) that can engage in interactions necessary for activation. The ethanol 2-carbon (methane = 38 cm^3/mol), xenon(43 cm^3/mol), nitrous oxide(35 cm^3/mol), and cyclopropane(63 cm^3/mol) are likely too small; propofol(639.5 cm^3/mol) and etomidate(835.5 cm^3/mol) are likely too large(Firestone, 1986). Carbon tetraiodide may fail to activate due to size constraints, however, aqueous solubility, degradation, and/or simultaneous TASK-3 inhibition may also be a factor. α-chloralose possesses a trichloromethane substituent sufficient for activation in other contexts (e.g., carbon tetrachloride, chloroform, trichloroethanol, and chloral hydrate), however, the large, water soluble carbohydrate substitution may sterically impair access to the activation site, favor hydration in water, and/or cause TASK-3 inhibition.

Molecular Pharmacology Fast Forward. Published on March 21, 2017 as DOI: 10.1124/mol.117.108290
This article has not been copyedited and formatted. The final version may differ from this version.

The anesthetic binding site -- We identified several missense mutants that impair TASK-3 activation at residues-122, -133, -136, -140, and one mutant that enhances it (residues-139) (Fig. 5 and Supplementary Fig. S3). The simplest interpretation is that these residues have a direct or near direct role in anesthetic binding; and the mutations that diminish activation, diminish interactions with the anesthetic and/or introduce a residue that sterically or electrostatically exclude it. Also and alternatively, introduction of a polar residue may favor water occupancy of the binding site over an anesthetic. Enhancing mutations might have the opposite effect.

Mutations, however, may also have an indirect, allosteric effect, and modify the binding site from afar, and/or modify channel gating (i.e., its open state probability) such that the functional consequences of binding are minimized or enhanced. For example, a channel that is "locked open" can not be further activated, whether it is binding an anesthetic or not. Crystal structures of TRAAK channels with a single activating mutation in the P-loop alpha helix have significant alterations in protein structure remote from the mutation site(Lolicato et al., 2014).

The results of the TASK-3 L122D mutation are novel as mutations in this region of TASK-3 have never been shown to modify anesthetic activation. Leu-122 in our homology model resides in the TASK-3 pore adjacent to the fenestration and in proximity to Leu-239 of the adjacent subunit (Fig. 1). Polar mutations at an equivalent residue in TWIK-1 (Leu-146) activate TWIK-1, and molecular dynamic studies suggest mutations here alter pore hydration and/or alter lipid access into the pore through the fenestration(Aryal et al., 2014; Aryal et al., 2015). Hydrophobic gating is a property of hydrophobic nanopores and hydration allows ions to conduct through the pore; and, as others have proposed, anesthetic agents may modify hydrophobic gating (Roth et al., 2008). The L122D mutation may eliminate hydrophobic gating

Molecular Pharmacology Fast Forward. Published on March 21, 2017 as DOI: 10.1124/mol.117.108290
This article has not been copyedited and formatted. The final version may differ from this version.

effects and thus anesthetic effects on hydrophobic gating. TREK-2 binds norfluoxetine in its hydrophobic fenestration(Dong et al., 2015). Likewise, TASK-3 may also bind anesthetics in its fenestration(Poulsen and Nissen, 2012), which would prevent lipids from accessing and blocking the pore; and L122D may disrupt both anesthetic fenestration binding and lipid pore entry(Brohawn et al., 2014). However, TASK-3 L122D is resistant to activation by both anesthetics and NEM-modification of Cys-159 and to inhibition by m3 GPCR activation, all similar to that seen previously in the TASK-3/TREK-1 mutant(Conway and Cotten, 2012; Talley and Bayliss, 2002). These observations suggests that Leu-122 has a critical role in TASK-3 gating, and we speculate that the L122D mutation stabilizes an open conformation promoted by anesthetic binding near Val-136 in the wild-type channel. TASK-3 V136E, although resistant to TCE and isoflurane activation, itself retains near wild-type sensitivity to m3 GPCR inhibition (Fig. 8). This implies that the V136E mutation, relative to L122D, has less effects on TASK-3 gating and a potentially greater role in anesthetic binding. N133D, like L122D and similarly resistant to m3 GPCR inhibition (Fig. 8), may also have gating effects.

A common mechanism of action and a technical advance -- TASK-3 mutants resistant to activation by TCE are also resistant to activation by isoflurane. This was true for L122D, M159W, and V136E. Though not definitive, this is consistent with both agents activating TASK-3 through a common mechanism. Therefore, results determined with one agent likely apply to both pending verification. Our results are also a technical advance in the study of TASK-3 anesthetic pharmacology. Because volatile anesthetics volatilize, they are difficult to handle and to apply in a quantitative manner particularly for prolonged periods. Halogenated alcohols, relative to volatile agents, have lower vapor pressures and increased aqueous solubility and can be handled in a more routine fashion with less concern for evaporative losses. This

Molecular Pharmacology Fast Forward. Published on March 21, 2017 as DOI: 10.1124/mol.117.108290
This article has not been copyedited and formatted. The final version may differ from this version.

property enabled TBE studies on yeast growth over the time course of days and sets the stage for high throughput and simultaneous screening of multiple TASK-3 and other tandem pore channel mutants.

Future studies and implications -- Future studies might address the potency and efficacy of the brominated agents in activating other members of the tandem pore family. With their potency and ease of handling, the brominated compounds (TBE and CBr_4) may be useful in crystallography studies or in developing a high potency, non-volatile photolabel for selective photolabeling of TASK-3 binding site residues. In the end, a better understanding of TASK channel activation will guide rational design of potent and selective activators. TASK activators may have clinical utility as sedative hypnotics. TASK channels have a putative role in hypoxia sensing in the carotid body and in the pulmonary artery, and activators also may have utility in managing the adverse cardiovascular sequelae of sleep apnea and chronic hypoxia, and in treating pulmonary hypertension.

Molecular Pharmacology Fast Forward. Published on March 21, 2017 as DOI: 10.1124/mol.117.108290
This article has not been copyedited and formatted. The final version may differ from this version.

Acknowledgements: The authors thank Drs. Richard Gaber (Northwestern) and Dan Minor (UCSF) for supplying yeast reagents and for guidance in their use, and Dr. Dan Bolon (UMass) for helpful a helpful discussion on yeast selection and next generation sequencing. LyTASK cDNA was provided by Dr. Nick Franks (Imperial College). The authors also thank their MGH colleagues Drs. Brijesh Bhayana, Hua-Jun Feng, Stuart Forman, Youssef Jounaidi, Keith Miller, and Douglas Raines for helpful discussions.

Authorship Contributions

Participated in research design: Luethy, Boghosian, Cotten.

Conducted experiments: Luethy, Boghosian, Cotten.

Contributed new reagents or analytic tools: Luethy, Boghosian, Cotten.

Performed data analysis: Luethy, Cotten.

Wrote or contributed to the writing of the manuscript: Luethy, Boghosian, Srikantha, Cotten.

Molecular Pharmacology Fast Forward. Published on March 21, 2017 as DOI: 10.1124/mol.117.108290
This article has not been copyedited and formatted. The final version may differ from this version.

References

Andres-Enguix I, Caley A, Yustos R, Schumacher MA, Spanu PD, Dickinson R, Maze M and Franks NP (2007) Determinants of the anesthetic sensitivity of TASK channels: molecular cloning of an anesthetic-activated potassium channel from Lymnaea stagnalis. *J Biol Chem* **282**(29): 20977-20990.

Aryal P, Abd-Wahab F, Bucci G, Sansom MS and Tucker SJ (2014) A hydrophobic barrier deep within the inner pore of the TWIK-1 K2P potassium channel. *Nat Commun* **5**: 4377.

Aryal P, Abd-Wahab F, Bucci G, Sansom MS and Tucker SJ (2015) Influence of lipids on the hydrophobic barrier within the pore of the TWIK-1 K2P channel. *Channels (Austin)* **9**(1): 44-49.

Bagriantsev SN and Minor DL, Jr. (2013) Using yeast to study potassium channel function and interactions with small molecules. *Methods Mol Biol* **995**: 31-42.

Bertaccini EJ, Dickinson R, Trudell JR and Franks NP (2014) Molecular modeling of a tandem two pore domain potassium channel reveals a putative binding site for general anesthetics. *ACS Chem Neurosci* **5**(12): 1246-1252.

Bertaccini EJ, Trudell JR and Franks NP (2007) The common chemical motifs within anesthetic binding sites. *Anesth Analg* **104**(2): 318-324.

Brohawn SG, Campbell EB and MacKinnon R (2014) Physical mechanism for gating and mechanosensitivity of the human TRAAK K+ channel. *Nature* **516**(7529): 126-130.

Brohawn SG, del Marmol J and MacKinnon R (2012) Crystal structure of the human K2P TRAAK, a lipid- and mechano-sensitive K+ ion channel. *Science* **335**(6067): 436-441.

Cadwell RC and Joyce GF (2006) Mutagenic PCR. *CSH Protoc* **2006**(1).

Chokshi RH, Larsen AT, Bhayana B and Cotten JF (2015) Breathing Stimulant Compounds Inhibit TASK-3 Potassium Channel Function Likely by Binding at a Common Site in the Channel Pore. *Mol Pharmacol* **88**(5): 926-934.

Conway KE and Cotten JF (2012) Covalent modification of a volatile anesthetic regulatory site activates TASK-3 (KCNK9) tandem-pore potassium channels. *Mol Pharmacol* **81**(3): 393-400.

Dong YY, Pike AC, Mackenzie A, McClenaghan C, Aryal P, Dong L, Quigley A, Grieben M, Goubin S, Mukhopadhyay S, Ruda GF, Clausen MV, Cao L, Brennan PE, Burgess-Brown NA, Sansom MS, Tucker SJ and Carpenter EP (2015) K2P channel gating mechanisms revealed by structures of TREK-2 and a complex with Prozac. *Science* **347**(6227): 1256-1259.

Firestone LL, Miller, J.C., Miller, K.W. (ed) (1986) *Tables of Physical and Pharmacological Properties of Anesthetics*, New York and Longdon.

Franks NP (2008) General anaesthesia: from molecular targets to neuronal pathways of sleep and arousal. *Nat Rev Neurosci* **9**(5): 370-386.

Franks NP and Lieb WR (1988) Volatile general anaesthetics activate a novel neuronal K+ current. *Nature* **333**(6174): 662-664.

Gruss M, Bushell TJ, Bright DP, Lieb WR, Mathie A and Franks NP (2004) Two-pore-domain K+ channels are a novel target for the anesthetic gases xenon, nitrous oxide, and cyclopropane. *Mol Pharmacol* **65**(2): 443-452.

Harinath S and Sikdar SK (2004) Trichloroethanol enhances the activity of recombinant human TREK-1 and TRAAK channels. *Neuropharmacology* **46**(5): 750-760.

Heurteaux C, Guy N, Laigle C, Blondeau N, Duprat F, Mazzuca M, Lang-Lazdunski L, Widmann C, Zanzouri M, Romey G and Lazdunski M (2004) TREK-1, a K+ channel involved in neuroprotection and general anesthesia. *Embo J* **23**(13): 2684-2695.

Honemann CW, Washington J, Honemann MC, Nietgen GW and Durieux ME (1998) Partition coefficients of volatile anesthetics in aqueous electrolyte solutions at various temperatures. *Anesthesiology* **89**(4): 1032-1035.

Kindler CH, Yost CS and Gray AT (1999) Local anesthetic inhibition of baseline potassium channels with two pore domains in tandem. *Anesthesiology* **90**(4): 1092-1102.

Krasowski MD, Finn SE, Ye Q and Harrison NL (1998) Trichloroethanol modulation of recombinant GABAA, glycine and GABA rho 1 receptors. *J Pharmacol Exp Ther* **284**(3): 934-942.

Krasowski MD and Harrison NL (2000) The actions of ether, alcohol and alkane general anaesthetics on GABAA and glycine receptors and the effects of TM2 and TM3 mutations. *Br J Pharmacol* **129**(4): 731-743.

Lazarenko RM, Willcox SC, Shu S, Berg AP, Jevtovic-Todorovic V, Talley EM, Chen X and Bayliss DA (2010) Motoneuronal TASK channels contribute to immobilizing effects of inhalational general anesthetics. *J Neurosci* **30**(22): 7691-7704.

Lolicato M, Riegelhaupt PM, Arrigoni C, Clark KA and Minor DL, Jr. (2014) Transmembrane helix straightening and buckling underlies activation of mechanosensitive and thermosensitive K(2P) channels. *Neuron* **84**(6): 1198-1212.

Miller AN and Long SB (2012) Crystal structure of the human two-pore domain potassium channel K2P1. *Science* **335**(6067): 432-436.

Nakamura RL and Gaber RF (1998) Studying ion channels using yeast genetics. *Methods Enzymol* **293**: 89-104.

Pang DS, Robledo CJ, Carr DR, Gent TC, Vyssotski AL, Caley A, Zecharia AY, Wisden W, Brickley SG and Franks NP (2009) An unexpected role for TASK-3 potassium channels in network oscillations with implications for sleep mechanisms and anesthetic action. *Proc Natl Acad Sci U S A* **106**(41): 17546-17551.

Parelkar NK, Silswal N, Jansen K, Vaughn J, Bryan RM, Jr. and Andresen J (2010) 2,2,2-trichloroethanol activates a nonclassical potassium channel in cerebrovascular smooth muscle and dilates the middle cerebral artery. *J Pharmacol Exp Ther* **332**(3): 803-810.

Patel AJ, Honore E, Lesage F, Fink M, Romey G and Lazdunski M (1999) Inhalational anesthetics activate two-pore-domain background K+ channels. *Nat Neurosci* **2**(5): 422-426.

Pettersen EF, Goddard TD, Huang CC, Couch GS, Greenblatt DM, Meng EC and Ferrin TE (2004) UCSF Chimera--a visualization system for exploratory research and analysis. *J Comput Chem* **25**(13): 1605-1612.

Poulsen H and Nissen P (2012) Structural biology. The inner workings of a dynamic duo. *Science* **335**(6067): 416-417.

Putzke C, Wemhoner K, Sachse FB, Rinne S, Schlichthorl G, Li XT, Jae L, Eckhardt I, Wischmeyer E, Wulf H, Preisig-Muller R, Daut J and Decher N (2007) The acid-sensitive potassium channel TASK-1 in rat cardiac muscle. *Cardiovasc Res* **75**(1): 59-68.

Roth R, Gillespie D, Nonner W and Eisenberg RE (2008) Bubbles, gating, and anesthetics in ion channels. *Biophysical journal* **94**(11): 4282-4298.

Sheppard DN, Carson MR, Ostedgaard LS, Denning GM and Welsh MJ (1994) Expression of cystic fibrosis transmembrane conductance regulator in a model epithelium. *Am J Physiol* **266**(4 Pt 1): L405-413.

Talley EM and Bayliss DA (2002) Modulation of TASK-1 (Kcnk3) and TASK-3 (Kcnk9) potassium channels: volatile anesthetics and neurotransmitters share a molecular site of action. *J Biol Chem* **277**(20): 17733-17742.

Winegar BD and Yost CS (1998) Activation of single potassium channels in rat cerebellar granule cells by volatile anesthetics. *Toxicol Lett* **100-101**: 287-291.

Yost CS (2003) Update on tandem pore (2P) domain K+ channels. *Curr Drug Targets* **4**(4): 347-351.

Molecular Pharmacology Fast Forward. Published on March 21, 2017 as DOI: 10.1124/mol.117.108290
This article has not been copyedited and formatted. The final version may differ from this version.

Footnotes

This research was supported the Massachusetts General Hospital Department of Anesthesia, Critical Care & Pain Medicine; the National Institutes of Health National Heart Lung and Blood Institute [Grant R01HL117871]; and Kantonsspital Aarau, Aarau, Switzerland (1410.000.062).

Molecular Pharmacology Fast Forward. Published on March 21, 2017 as DOI: 10.1124/mol.117.108290
This article has not been copyedited and formatted. The final version may differ from this version.

Figure Legends

Figure 1. A, homology model of TASK-3 potassium channel (spanning residues Gln-4 to Val-243) with relevant residues indicated: Leu-122 (red), Met-133 (red), Val-136 (orange), Leu-139 (green), Leu-140 (yellow), Met-159 (blue), Leu-239 (green), Leu-241 (magenta), Leu-242 (black), Val-243 (purple), and four potassium ions in the selectivity filter (green). M1-4 and m2-4 indicate the transmembrane domains 1-4 and 2-4 in apposing TASK-3 subunits, respectively. B, bottom/cytoplasmic view achieved by rotating the structure in A first 90º then 35º along its x- and y-axes, respectively. The surface rendering is transected through the putative anesthetic binding pocket (perforated red line) and the pore fenestration (blue perforated arrow). A 5 angstrom (Å) scale bar is provided in A and B.

Figure 2. A, chemical structure of clinically relevant agents used in this study. B, chemical structures of some halogenated ethanol and methane drugs/compounds used in this study: TBE, 2,2,2-tribromoethanol; TCE, 2,2,2-trichloroethanol; TFE, 2,2,2-trifluoroethanol; EtOH, ethanol; CI_4, carbon tetraiodide; CBr_4, carbon tetrabromide; CCl_4, carbon tetrachloride; and HFP, 1,1,1,3,3,3-hexafluoro-2-propanol. C, illustration of relative sizes of iodofrom ($CHCI_3$), bromoform ($CHBr_3$), chloroform ($CHCl_3$), fluoroform (CHF_3), and 1,1,1,3,3,3-hexafluoro-2-propane. A 5 angstrom (Å) scale bar (in light blue), estimated volume (in cm^3/mol), average molecular polarizability (in $Å^3$), and calculated lipophilicity (XlogP) are provided.

Figure 3. TASK-3 channel function is activated by brominated and chlorinated methanes and alcohols. A, Ussing chamber potassium current records using Fischer rat thyroid cell monolayers expressing wild-type TASK-3 channels. Downward arrows indicate study compound application; perforated lines, zero current level; 'L' shaped bars, current (in μA) and

Molecular Pharmacology Fast Forward. Published on March 21, 2017 as DOI: 10.1124/mol.117.108290
This article has not been copyedited and formatted. The final version may differ from this version.

time scale; and white bars, acidic pH. In each, transmonolayer voltage was clamped at 0 mV; intermittent +5 mV pulses assess membrane integrity. B, normalized, steady-state concentration-response of wild-type TASK-3 to EtOH, isoamyl alcohol, TFE, MCE, DCE, TCE, TBE, CCl_4, CBr_4 and CI_4. n = from 3 to 8 for each ± SD. Data were normalized to baseline current. Data for TCE, TBE, CCl_4, and CBr_4 , which caused clear activation, were fit with the following: Y = 100 + (I_{max}-100)/(1+10^(($Log_{10}EC_{50}$-X)*HillSlope)) in which I_{max} = maximum normalized current, and X = Log_{10}[activating agent]. TCE, TBE, CCl_4, and CBr_4 data, respectively, for **I_{max} (in %; 95% confidence)**: 215(196 to 234), 267(240 to 294), 180(163 to 196), and 296(245 to 346). **EC_{50} (in μM):** 1077(647 to 793), 295(195 to 447), 289(170 to 492), and 16(7 to 37). **HillSlope:** 1.0 (0.5 to 1.4), 1.1(0.8 to 1.4), 1.7 (0.7 to 2.7), and 1.2 (0.2 to 2.2). Data points for other non-activating agents are connected with a straight line.

Figure 4. TASK-3 channel function is activated by multiple clinically relevant halogenated agents. A, Ussing chamber potassium current records using Fischer rat thyroid cell monolayers expressing wild-type TASK-3 channels. Data were collected as described in Fig. 3 with n = 3 to 5 ± SD for each. B, concentration-response for halothane, isoflurane, desflurane, sevoflurane, hexafluoropropanol (HFP), chloral hydrate, and α-chloralose. Data points were fitted as in Fig. 3. Chloral hydrate, isoflurane, desflurane, sevoflurane, and HFP data, respectively, for **I_{max} (in %; 95% confidence)** = 165(161 to 170), 169(161 to 176), 119(109 to 129), 164(150 to 177), and 200(194 to 206). **EC_{50} (in μM):** 7141(6386 to 7986), 363(283 to 466), 433(179 to 1047), 265(181 to 38) and 1942(1683 to 2241). **HillSlope:** 2.0(1.7 to 2.3), 1.5(1.0 to 2.0), 1.7(-0.8 to 4.3), 1.4 (0.8 to 2.1), and 1.6(1.3 to 1.9).

Figure 5. Effects of TASK-3 residue-136 and adjacent residue mutagenesis on 2,2,2-

Molecular Pharmacology Fast Forward. Published on March 21, 2017 as DOI: 10.1124/mol.117.108290
This article has not been copyedited and formatted. The final version may differ from this version.

trichloroethanol (TCE) activation. A, representative current records from FRT monolayers expressing TASK-3 N133D, L140D, V136I, V136W, V136K, and V136E. Details of currents records are as described in Fig. 3. B, compiled TCE concentration-response for multiple TASK-3 mutants. Data points were fitted as described in Fig. 3. For mutants **V136A, V136G, V136I, V136S, V136D,** respectively, **I_{max} (in %; 95% confidence):** 129(123 to 134), 117(115 to 120), 198(177 to 220), 130(124 to 137), 139(63 to 216). **EC_{50} (in μM):** 977(566 to 1687), 1188(841 to 1679), 3867(2308 to 6477), 4900(3478 to 6904), 13300(2290 to 77260). **HillSlope:** 1.3(0.4 to 2.1), 3.0 (0.2 to 5.8), 1.2(0.8 to 1.6), 2.1(1.0 to 3.1), 2.7 (-2.7 to 8.1). For mutants **M132D, T134D, F135D, R137D, Y138D, L139D**, respectively, **I_{max} (in %; 95% confidence):** 180(162 to 199), 251(239 to 264), 149(146 to 153), 178(173 to 184), 211(201 to 221), 300(280 to 320). **EC_{50} (in μM):** 6084(4587 to 8070), 1297(1036 to 1623), 782(636 to 961), 888(732 to 1077), 1351(1035 to 1762), 869(661 to 1143). **HillSlope:** 3.2(0.7 to 5.6), 1.3(0.9 to 1.6), 1.6(1.0 to 2.1), 1.5(1.0 to 1.9), 1.1 (0.8 to 1.4), 1.7(0.9 to 2.5). C, relevant segment of the TASK-3 homology model (residues Met-132 through Leu-140) to illustrate the predicted three dimensional relationship of the residue side chains.

Figure 6. TASK-3 mutants L122D, V136E, and M159W disrupt TCE and isoflurane activation. A, currents records from FRT monolayers expressing TASK-3 M159W and L122D and their response to TCE or isoflurane. Details of currents records are as described in Fig. 3. B, compiled TCE concentration-response for TASK-3 M159W, L122D, and V136E. Wild-type TASK-3 data are from Figs. 3 and 4. Data points for M159W, L122D, and V136E are connected by a straight line.

Figure 7. TASK-3 activation following Cys-159 covalent modification is impaired by

Molecular Pharmacology Fast Forward. Published on March 21, 2017 as DOI: 10.1124/mol.117.108290
This article has not been copyedited and formatted. The final version may differ from this version.

L122D and V136E. Currents records from FRT monolayers expressing TASK-3 M159C (A), M159C/V136E (B) and M159C/L122D (C) exposed to 5 mM NEM, a cysteine-selective alkylating agent. Details of currents records are as described in Fig. 3. D, peak steady-state normalized current following 5 mM NEM modification for M159C, M159C/V136E, and M159C/L122D. Data are fitted as in Fig. 3; n = at least 3± SD for each. Asterisks (***) indicate significance ($P < 0.001$) relative to TASK-3 M159C as determined by a one-way ANOVA and a post-hoc Bonferroni multiple comparison test.

Figure 8. TASK-3 L122D is resistant to m3 muscarinic G-protein coupled receptor (GPCR) regulation. A, currents records from FRT monolayers co-expressing m3 muscarinic GPCR and wild-type (A), V136E (B), and L122D (C) TASK-3 channels exposed to increasing concentrations of carbachol (downward arrows). Details of currents records are as described in Fig. 3. D, compiled carbachol concentration-response for L122D, N133D, L140D, wild-type, and V136E TASK-3 channels. n = at least 3 ± SD for each data point. Asterisks (*** and **) indicate significance ($P < 0.001$ and 0.01) relative to wild-type and V136E TASK-3 at 1 mM carbachol as determined by a one-way ANOVA and a post-hoc Bonferroni multiple comparison test.

Figure 9. TBE selects for *trk1Δtrk2Δ* potassium-sensitive yeast expressing "yeast optimized" wild-type (i.e., Val-136) TASK-3 over those expressing "yeast optimized" TASK-3 V136E (i.e., Glu-136) mutant. The Log_{10} ratio of residue-136 TASK-3 cDNA variants (Val-136/Glu-136) transformed yeast growth (quantified by A600) grown in the presence of DMSO (vehicle) or 1 mM TBE. Bars indicate mean ± SD; n = 4 samples each. TASK-3 cDNA was optimized for yeast functional expression as discussed in Methods. Relative frequency of each residue-136 variant in samples was counted by Illumina MiSeq DNA

Molecular Pharmacology Fast Forward. Published on March 21, 2017 as DOI: 10.1124/mol.117.108290
This article has not been copyedited and formatted. The final version may differ from this version.

sequencing. Sequence counts (Val-136/Glu-136) for all samples grown without TBE: 7541/11073, 4981/7036, 8157/10641, 11265/15075; sequence counts for samples grown with 1 mM TBE: 10630/5547, 14113/7440, 14633/8785, 14104/7630. Asterisks (***) indicate significance ($P < 0.001$) of Val-136/Glu-136 ratios from samples grown in the presence of 1 mM TBE relative to those grown in DMSO vehicle alone using an unpaired, two-tailed Student's t test.

Figure 10. Cartoon model of proposed 2,2,2-tribromoethanol interaction with the TASK-3 anesthetic binding site. The 2-carbon and its bromine atoms interacts with the anesthetic binding site with the 1-carbon hydroxyl excluded.

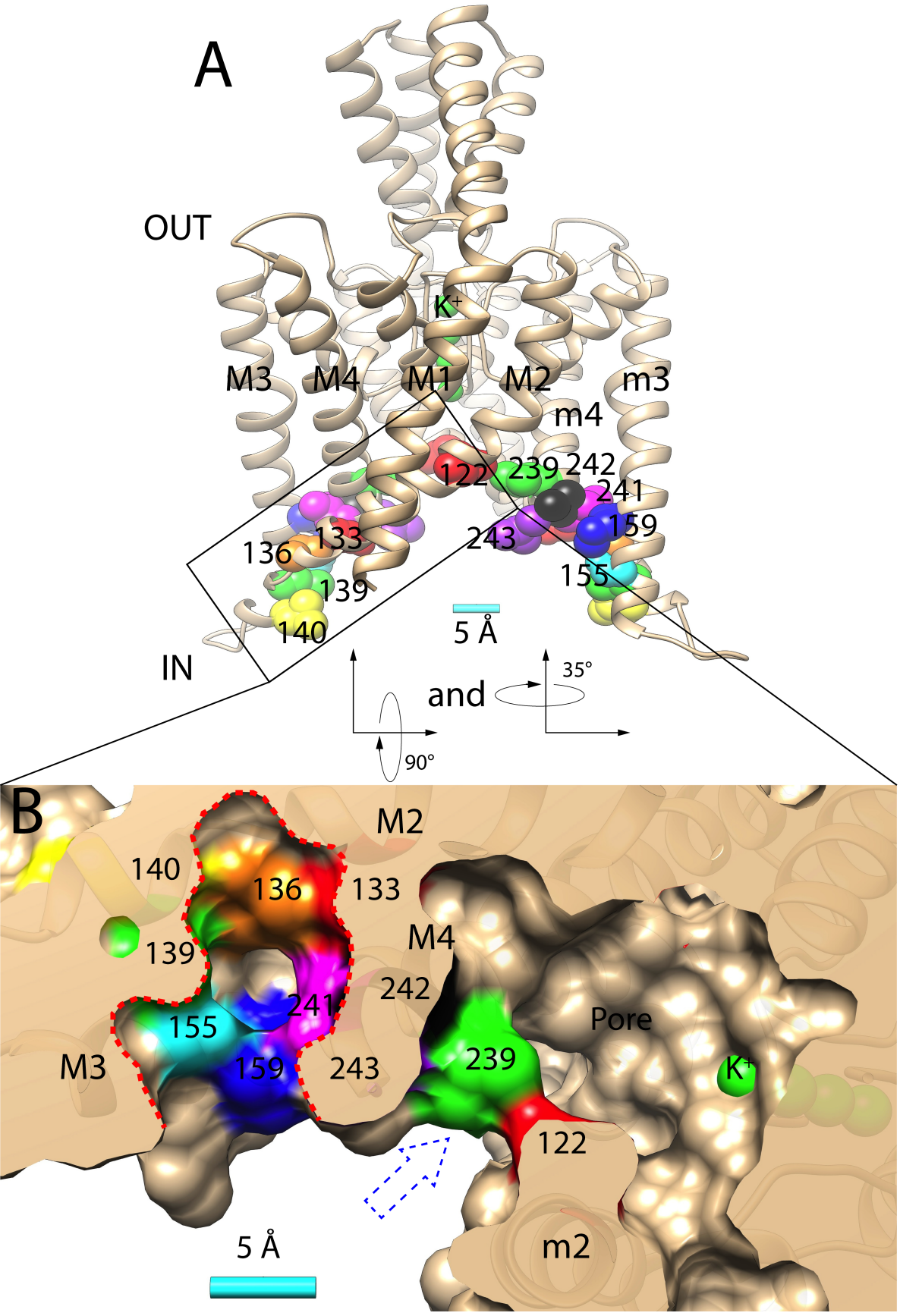
A
OUT
K+
M3
M4
M1
M2
m3
m4
122
239
242
241
159
243
133
136
155
139
140
5 Å
IN
and
35°
90°
B
M2
140
136
133
M4
139
242
241
Pore
155
M3
159
243
239
K+
122
5 Å
m2

Figure 1

Molecular Pharmacology Fast Forward. Published on March 21, 2017 as DOI: 10.1124/mol.117.108290
This article has not been copyedited and formatted. The final version may differ from this version.

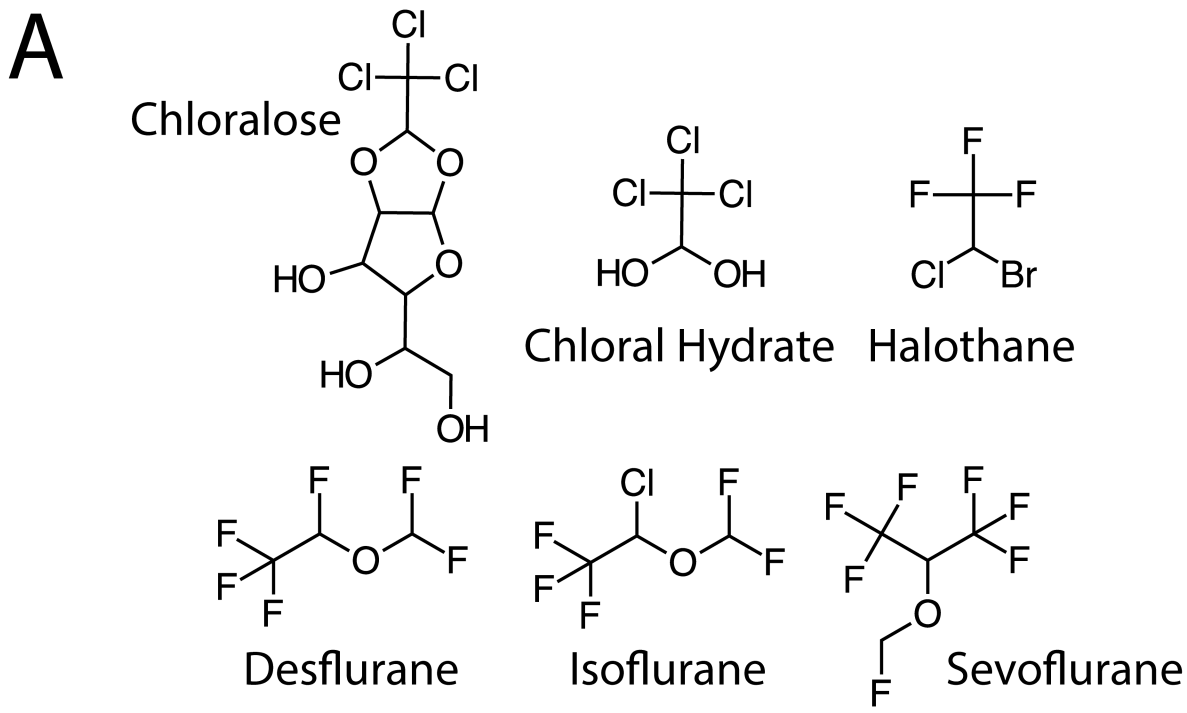

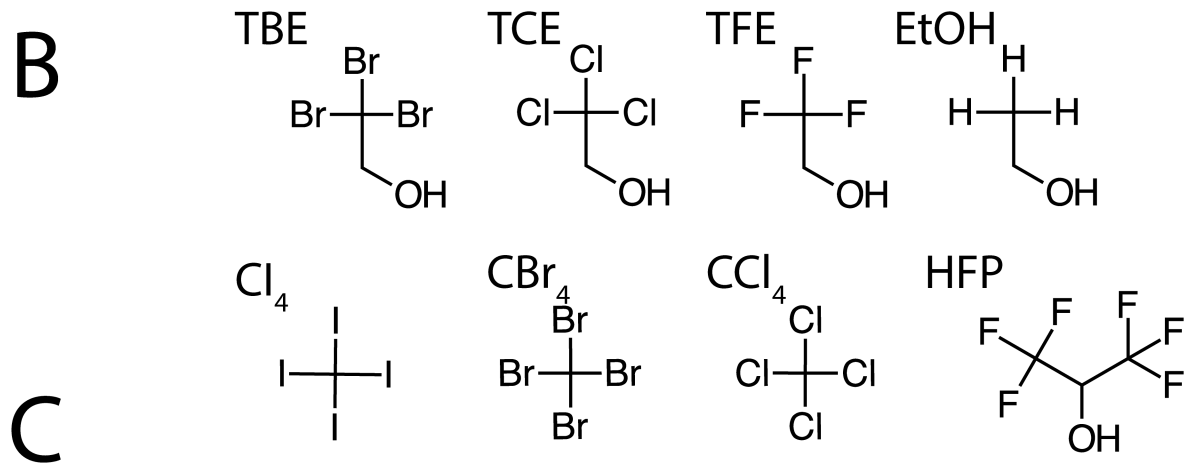

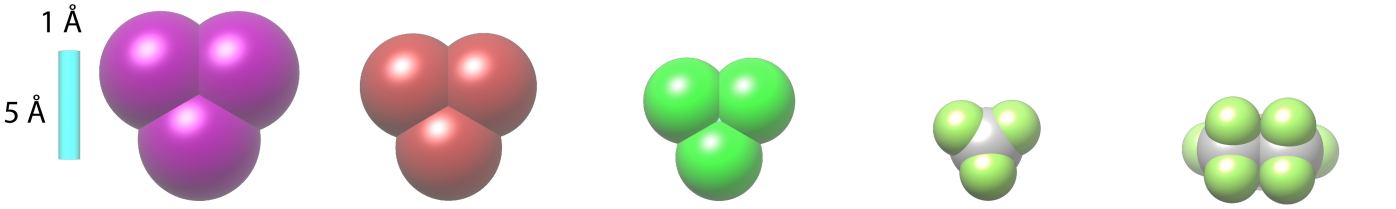

Iodoform(CHI_3)
232.0 cm^3/mol
18.072 $Å^3$
XlogP 3.688

Bromoform($CHBr_3$)
154.7 cm^3/mol
11.967 $Å^3$
XlogP 3.088

Chloroform($CHCl_3$)
91.86 cm^3/mol
8.5 $Å^3$
XlogP 2.074

Fluoroform(CHF_3)
30.31 cm^3/mol
2.795 $Å^3$
XlogP 1.663

Hexafluoro-
propane(CF_3CHCF_3)
71.47 cm^3/mol
6.591 $Å^3$
XlogP 3.418

Figure 2

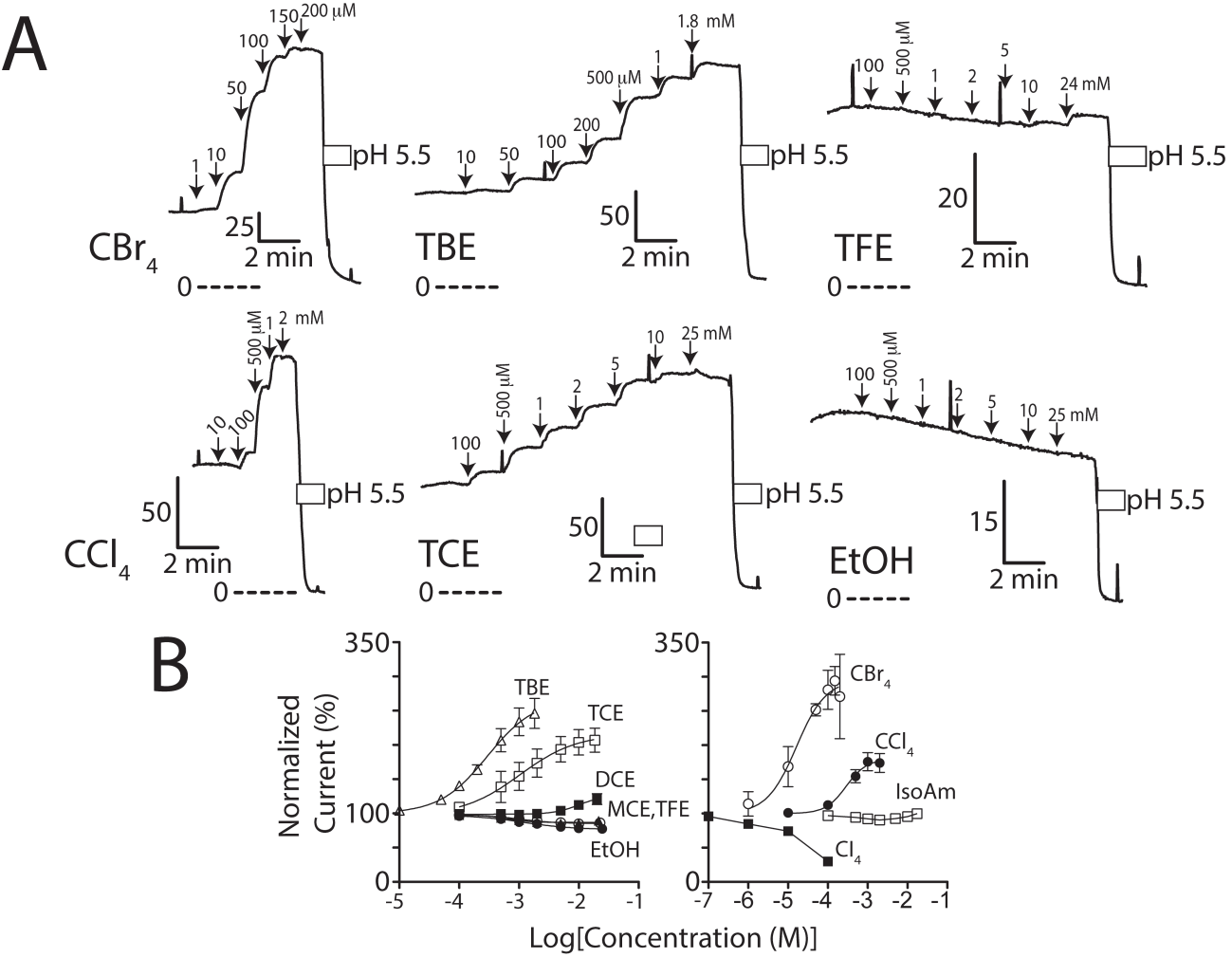

Figure 3

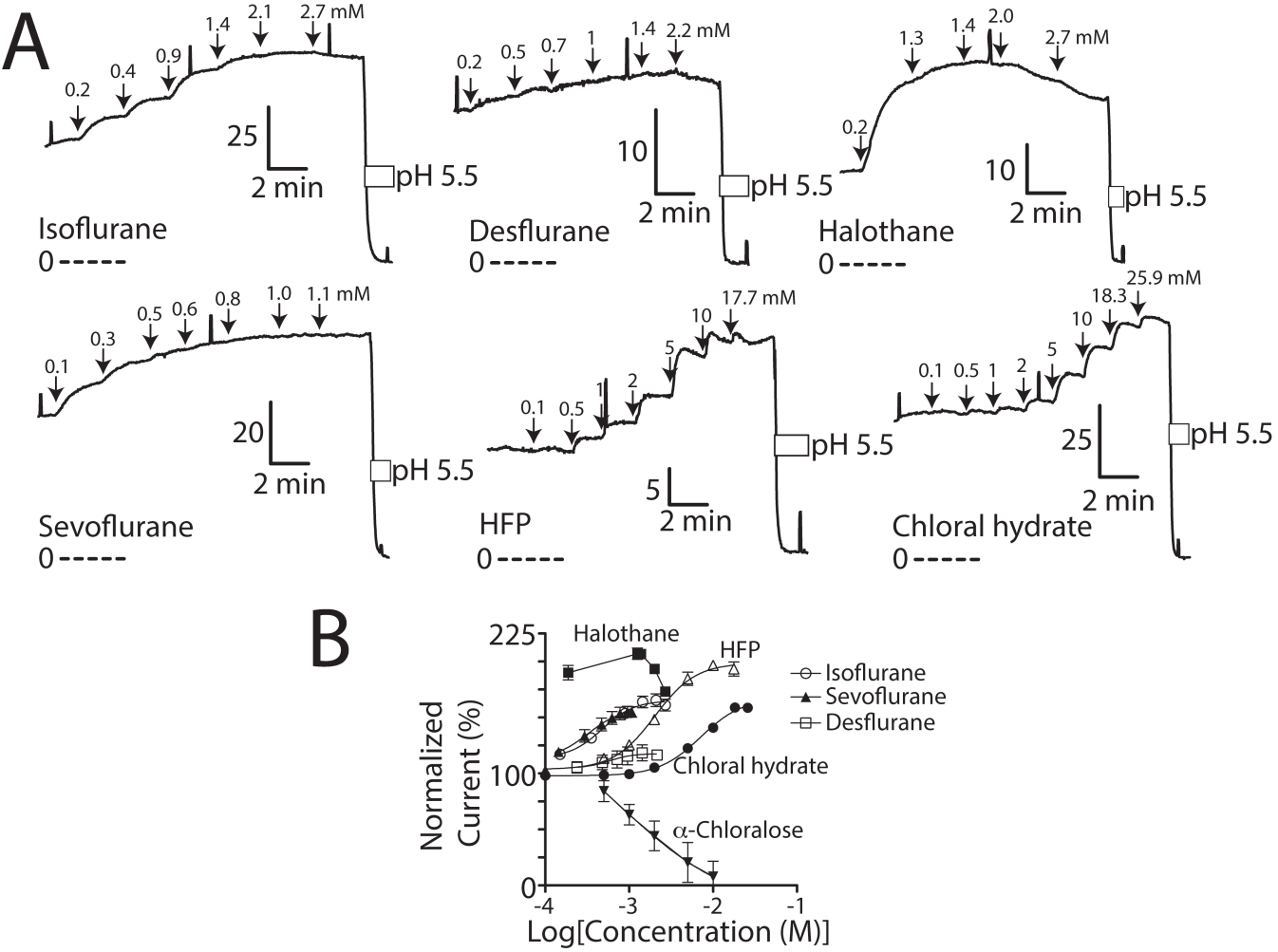

Figure 4

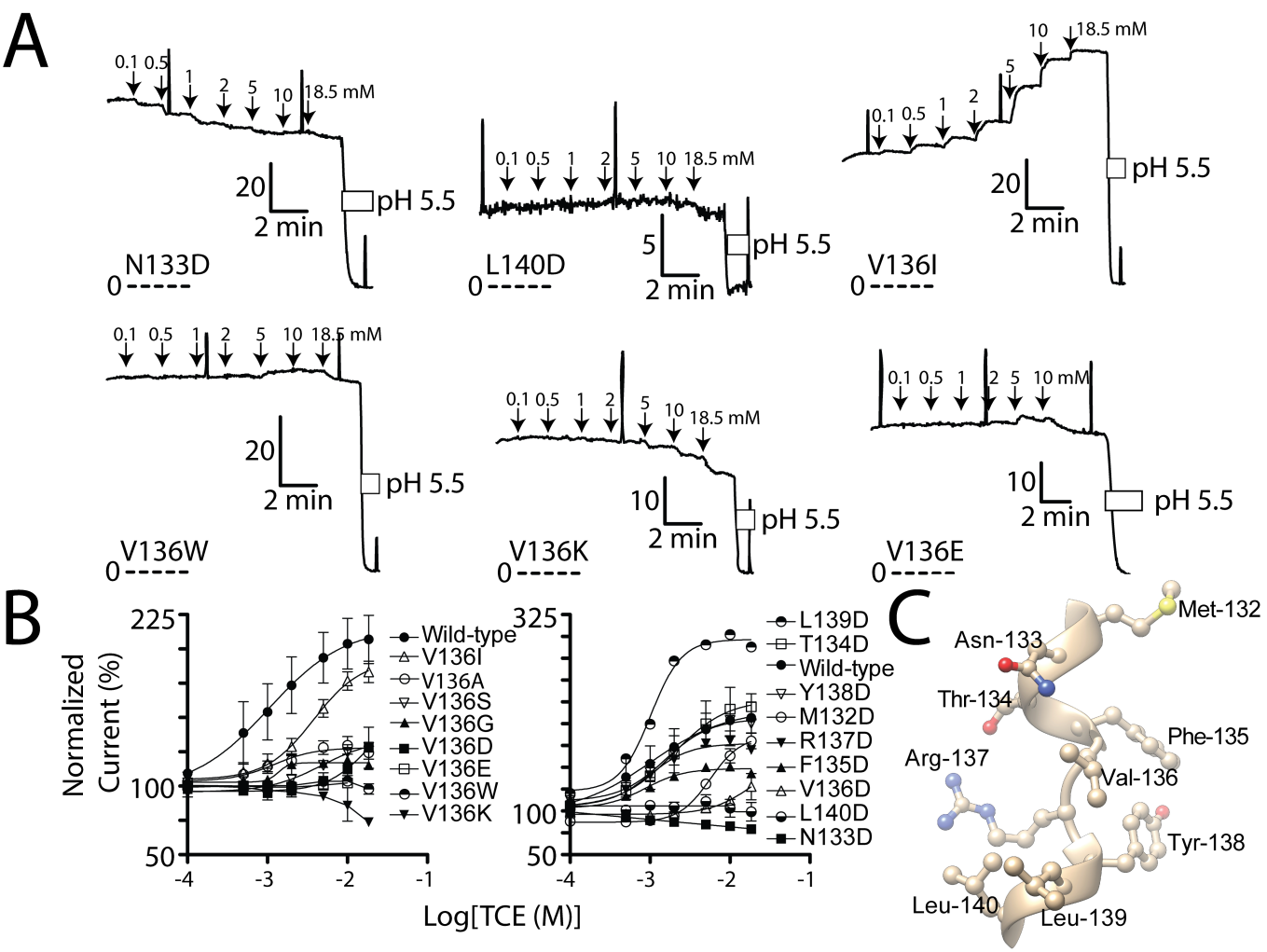

Figure 5

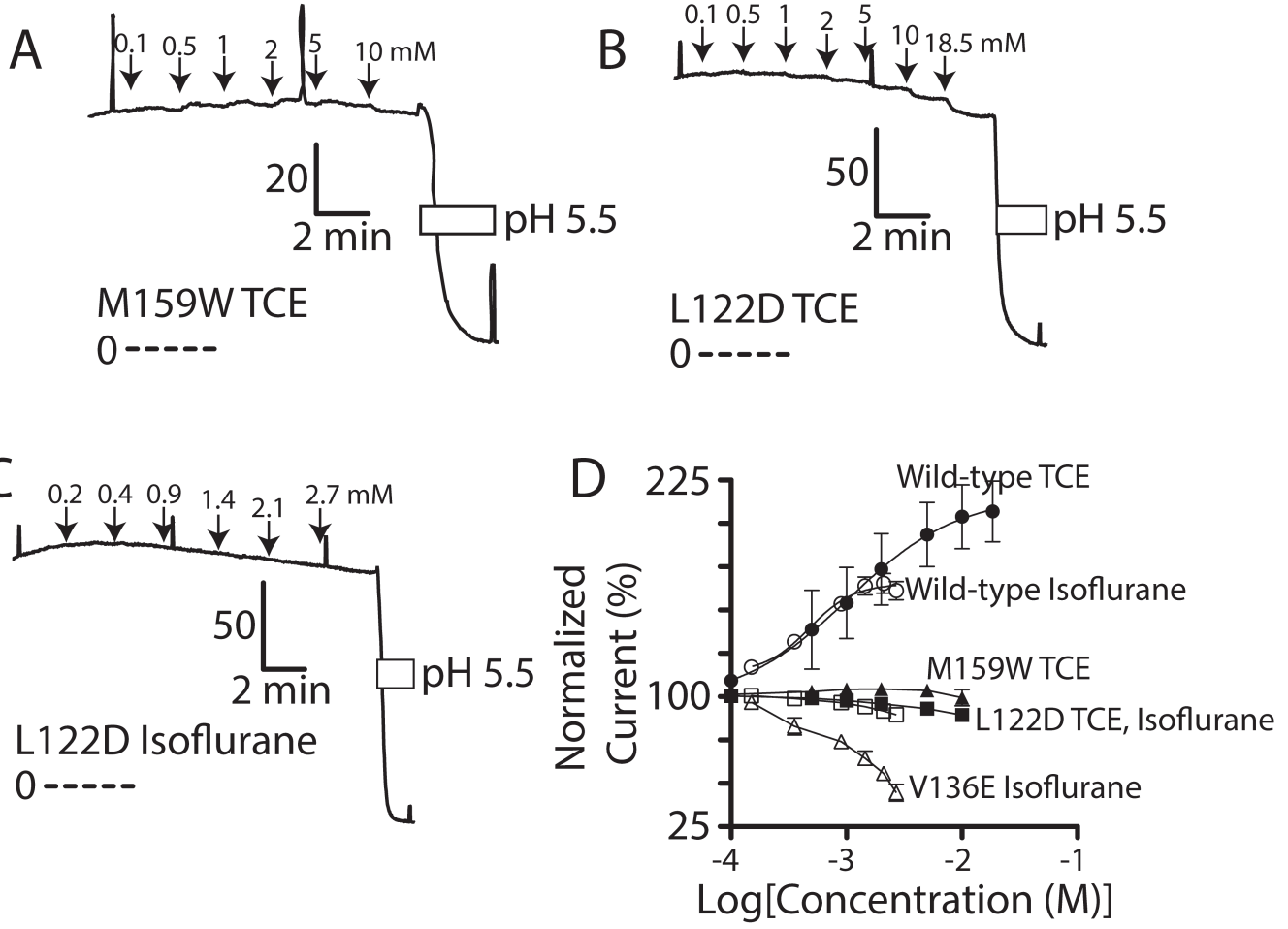
A
0.1 0.5 1 2 5 10 mM
20
2 min
pH 5.5
M159W TCE
0
B
0.1 0.5 1 2 5 10 18.5 mM
50
2 min
pH 5.5
L122D TCE
0
C
0.2 0.4 0.9 1.4 2.1 2.7 mM
50
2 min
pH 5.5
L122D Isoflurane
0
D
225
100
25
Normalized Current (%)
Wild-type TCE
Wild-type Isoflurane
M159W TCE
L122D TCE, Isoflurane
V136E Isoflurane
-4
-3
-2
-1
Log[Concentration (M)]

Figure 6

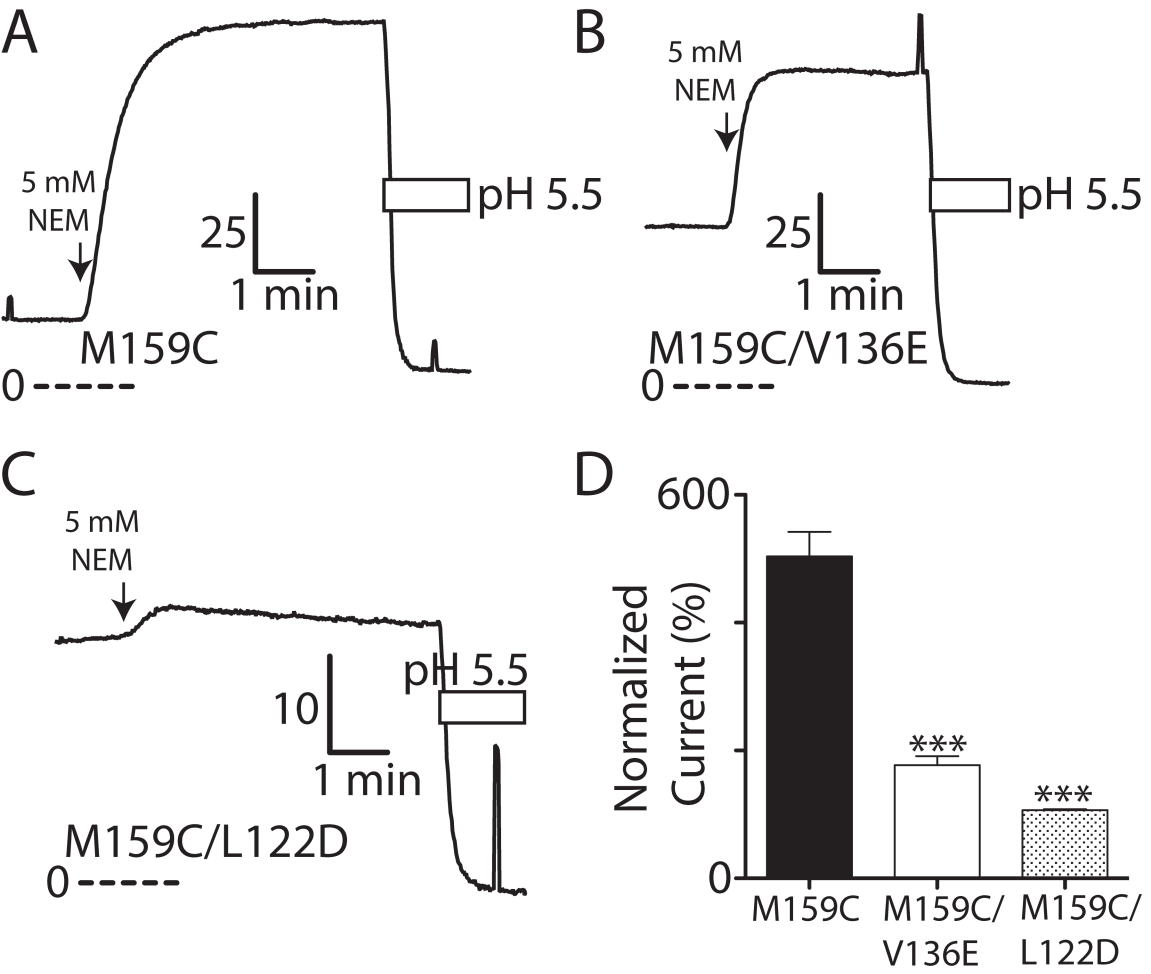
A
5 mM
NEM
pH 5.5
25
1 min
M159C
0
B
5 mM
NEM
pH 5.5
25
1 min
M159C/V136E
0
C
5 mM
NEM
pH 5.5
10
1 min
M159C/L122D
0
D
600
Normalized
Current (%)
0
***
***
M159C
M159C/
V136E
M159C/
L122D

Figure 7

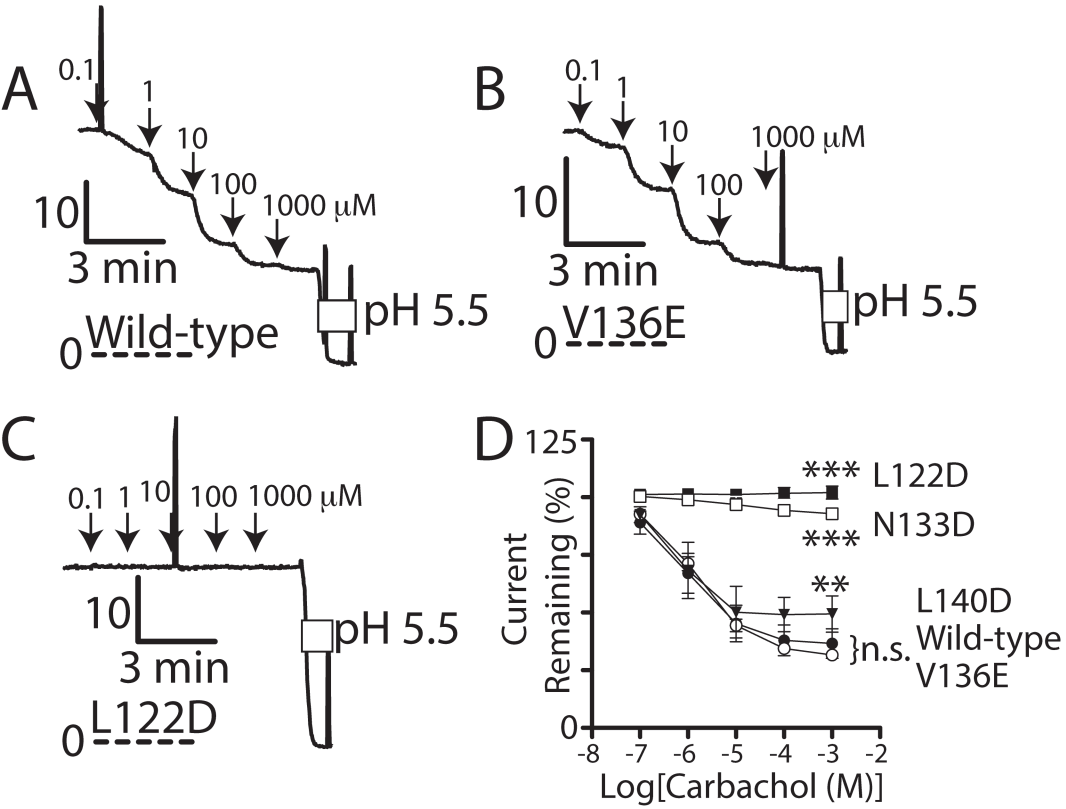
A
0.1
1
10
100
1000 μM
10
3 min
Wild-type
0
pH 5.5
B
0.1
1
10
100
1000 μM
10
3 min
V136E
0
pH 5.5
C
0.1 1 10 100 1000 μM
10
3 min
L122D
0
pH 5.5
D
125
Current Remaining (%)
0
-8 -7 -6 -5 -4 -3 -2
Log[Carbachol (M)]
*** L122D
*** N133D
** L140D
}n.s. Wild-type
V136E

Figure 8

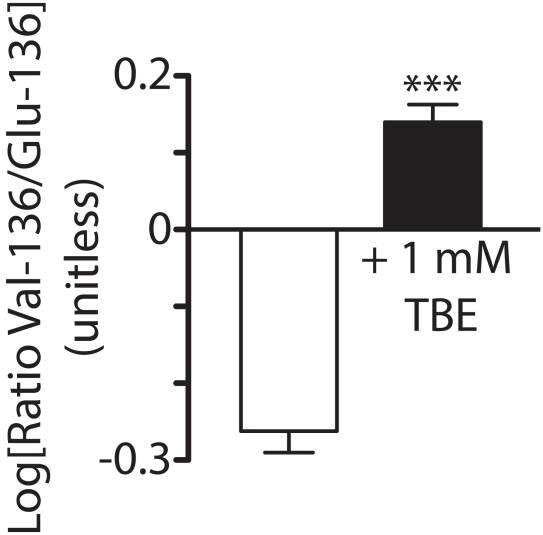

Figure 9

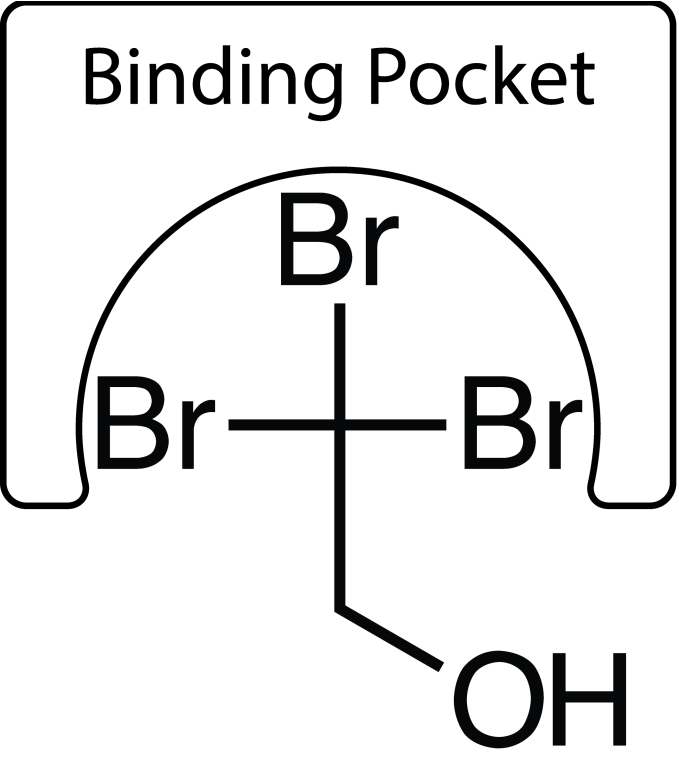

Figure 10